The prohormone VGF regulates β-cell function via insulin secretory granule biogenesis

Samuel B. Stephens[1,2,3,9], **Robert J. Edwards**[4], **Masato Sadahiro**[6,8], **Wei-Jye Lin**[6], **Cheng Jiang**[6,8], **Stephen R. Salton**[6,7], and **Christopher B. Newgard**[1,2,3,5]

[1]Sarah W. Stedman Nutrition and Metabolism Center, Durham, NC 27704, USA

[2]Duke Molecular Physiology Institute, Durham, NC 27704, USA

[3]Department of Pharmacology and Cancer Biology, Division of Endocrinology, Duke University Medical Center, Durham, NC 27704, USA

[4]Department of Cell Biology, Division of Endocrinology, Duke University Medical Center, Durham, NC 27704, USA

[5]Department of Medicine, Division of Endocrinology, Duke University Medical Center, Durham, NC 27704, USA

[6]Department of Neuroscience, Icahn School of Medicine at Mt. Sinai, New York City, New York 10029, USA

[7]Friedman Brain Institute, Icahn School of Medicine at Mt. Sinai, New York City, New York 10029, USA

[8]Graduate School of Biomedical Sciences, Icahn School of Medicine at Mt. Sinai, New York City, New York 10029, USA

Summary

The prohormone VGF is expressed in neuroendocrine and endocrine tissues and regulates nutrient and energy status both centrally and peripherally. We and others have shown that VGF-derived peptides have direct action on the islet β-cell as secretagogues and cytoprotective agents; however the endogenous function of VGF in the β-cell has not been described. Here we demonstrate that VGF regulates secretory granule formation. VGF loss of function studies in both isolated islets and conditional knockout mice reveal a profound decrease in stimulus-coupled insulin secretion. Moreover, VGF is necessary to facilitate efficient exit of granule cargo from the *trans*-Golgi

[9]Current address and lead contact: Samuel B Stephens, Ph.D., Fraternal Order of Eagles Diabetes Center, Department of Internal Medicine, Division of Endocrinology and Metabolism, University of Iowa, Iowa City, IA 52246, samuel-b-stephens@uiowa.edu, Tel. 319-335-4843

Author contributions

network and proinsulin processing. It also functions to replenish insulin granule stores following nutrient stimulation. Our data support a model in which VGF operates at a critical node of granule biogenesis in the islet β-cell to coordinate insulin biosynthesis with β-cell secretory capacity.

eTOC blurb

Stephens et al. find that the granin protein, VGF, regulates key aspects of pancreatic islet β-cell function. These studies highlight a role for VGF in the maintenance and replenishment of insulin granules during nutrient stimulation by promoting exit of granule cargo from the *trans*-Golgi network and facilitating granule formation.
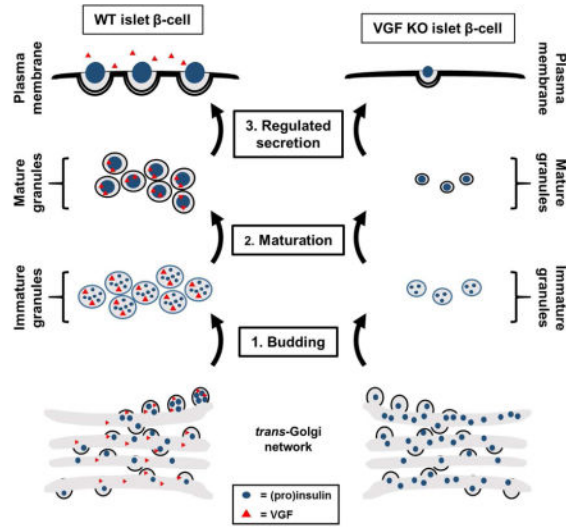
Keywords

VGF; secretory granule; insulin secretion; granule biogenesis; chromogranin B; β-cell function

Introduction

The regulated release of the pancreatic islet hormones glucagon and insulin from α- and β-cells, respectively, coordinates metabolic fuel homeostasis. Inappropriate islet hormone release, including insulinopenia due to loss of β-cell function and mass, and hyperglucagonemia from dysregulation of α-cell function interacts with insulin resistance to cause sustained hyperglycemia and the development of Type 2 diabetes (T2D). Multiple factors may contribute to the deterioration of islet cell function in T2D, including genetic predisposition, gluco-lipotoxicity, increased secretory demand, ER and oxidative stress, and inflammatory cytokines (Muoio and Newgard, 2008). Regardless of the destructive mechanism, maintenance of functional β-cell mass is recognized as a key strategy for delaying and/or preventing development of T2D.

The packaging of hormones such as glucagon and insulin into secretory vesicles for regulated (nutrient-coupled) secretion requires both positive and negative selection mechanisms (reviewed in Dikeakos and Reudelhuber, 2007). Distinct from other organelles,

proteins destined for regulated secretion lack well-defined (conserved) structural motifs. In a process termed "sorting for entry", protein cargo may be actively sorted into immature secretory granules (ISG) in the *trans*-Golgi network (Chung et al., 1989) via association with the clathrin-coated granule membrane (phogrin) (Wasmeier et al., 2002), binding to cholesterol-rich lipid raft microdomains (secretogranin III) (Hosaka et al., 2004), and/or putative sorting receptors (carboxypeptidase E) (Cool and Loh, 1998). In contrast, a negative selection mechanism called "sorting by retention" involves aggregation of proteins in the granule lumen to promote cargo retention during retrieval of proteins from ISGs not destined for regulated secretion (Arvan and Castle, 1998). Much attention has been paid to the granin proteins, chromogranin A (CgA) and chromogranin B (CgB), as key determinants of granule biogenesis, in part because these proteins comprise a major component of the secretory granule in multiple endocrine and neuroendocrine cell types (Helle, 2000). CgA has been suggested to play a key regulatory role in granule formation in some cell types (Kim et al., 2001, Kim et al., 2002), but its potential role in the islet β-cell is not well defined. Furthermore, conflicting studies from CgA knockout mice make the requirements for CgA in granule formation and maintenance in adrenal medullar chromaffin cells unclear (Hendy et al., 2006, Mahapatra et al., 2005, Diaz-Vera et al., 2012), and suggest the existence of alternative or redundant mechanisms. Recent studies using CgB KO mice have shown that CgB is an essential component of β-cell function (Obermuller et al., 2010). Islets isolated from CgB KO mice have impaired insulin release and elevated proinsulin secretion. However, a clear understanding of the contributions of CgA and CgB to insulin granule formation, and the identity of other potential regulatory factors, is still lacking.

VGF (non-acronymic; unrelated to VEGF) has emerged as a factor regulating whole animal metabolism in multiple tissues. Pro-VGF is expressed centrally in neuroendocrine cells of the hypothalamus and hippocampus and peripherally in endocrine tissues such as the adrenal medulla and pancreatic islet (α-, β- and δ–cells) (Cocco et al., 2007, Ferri et al., 1992, Possenti et al., 1999, Trani et al., 2002, van den Pol et al., 1989). Pro-VGF is packaged into dense core secretory granules with other hormones such as insulin (Ferri et al., 1992, Possenti et al., 1999, Gentile et al., 2004) and is proteolytically processed via PC1/3 and PC2 into a panel of secreted peptides (Trani et al., 2002, Possenti et al., 1999, Stephens et al., Pan et al., 2005). Much of our current understanding of endogenous VGF function has been derived from the targeted deletion of VGF in mice (Watson et al., 2005, Hahm et al., 1999, Hahm et al., 2002, Watson et al., 2009). VGF null mice are hypermetabolic (Hahm et al., 1999), demonstrate enhanced lipolysis (Fargali et al., 2012), and have reduced islet size and circulating insulin and glucose levels (Watson et al., 2005, Hahm et al., 1999). In multiple disease models (diet-induced obesity, *ob/ob*, $MC4R^{-/-}$), $VGF^{-/-}$ mice fail to develop obesity, hyperglycemia or hyperinsulinemia; rather these animals remain lean and insulin sensitive (Hahm et al., 2002, Watson et al., 2005). Presumably, secreted VGF peptides function as paracrine or endocrine hormones to engage with receptor-bearing target tissues. Indeed, we and others have demonstrated that VGF peptides can enhance β-cell function (Stephens et al., Petrocchi-Passeri et al., 2015, Moin et al.) and promote cell survival in multiple cell systems (Severini et al., 2008, Stephens et al.). Our previous work demonstrated that the C-terminal VGF peptide TLQP-21 enhances glucose-stimulated insulin secretion (GSIS) and promotes β-cell survival through a cAMP-mediated pathway

(Stephens et al.). However the possible functions of intracellular, endogenous VGF in islets cells has not been established.

Recent studies highlight a second, intracellular function for VGF as a granin protein involved in the process of granule formation (Fargali et al., 2014). Overexpression of VGF in non-endocrine cells induces granule formation, whereas loss of VGF reduces granule size in catecholaminergic chromaffin cells. Although VGF lacks sequence homology to other granins, VGF shares physical characteristics with other granin proteins including a series of dibasic (cleavage) residues scattered throughout the proprotein and importantly, the ability to aggregate under conditions of low pH and elevated Ca^{2+} (Bartolomucci et al., 2011, Fargali et al., 2014). Whether VGF plays a role in granule formation in other endocrine cell types such as pancreatic islets is not known.

In the current study, we demonstrate that suppression of VGF expression results in loss of β-cell secretory function due to a deficit in releasable insulin granules. In the absence of VGF, second phase stimulus-coupled insulin secretion is strongly impaired. This involves a reduction in the size and number of β-cell secretory granules and an accumulation of granule cargo including insulin, CgA and CgB near the *trans*-Golgi-network. In addition, there is a significant reduction in the rate of proinsulin processing and an impairment in the replenishment of insulin granule stores. Using a mouse model, we further show that β-cell specific knockout of VGF results in impaired glucose tolerance due to a reduction in circulating insulin. We propose that VGF acts as a central mediator in granule biogenesis to facilitate efficient granule formation in the islet β-cell.

Results

Loss of VGF impairs stimulated insulin release

VGF is a member of the granin family of proteins and has been suggested to contribute to granule biogenesis in endocrine tissues (Bartolomucci et al., 2011, Fargali et al., 2014, Gentile et al., 2004). VGF is highly expressed in pancreatic islet β-cells (Cocco et al., 2007) yet the potential function of VGF in the regulation of granule and insulin trafficking has not been formally investigated. To begin, we used siRNAs to suppress expression of VGF in the robustly glucose responsive 832/3 insulinoma cell line. As shown in Figure 1, an 80% decrease in VGF protein levels (Fig. 1B) caused by either of two distinct VGF siRNA duplexes, resulted in a greater than 50% decrease in GSIS (at 12 mM Glc) with no change observed at basal glucose levels (2.5 mM Glc) compared to either mock-transfected cells or cells transfected with a non-targeting siRNA (SCR) (Fig. 1A). Next, we investigated the ability of cAMP-raising agents to rescue the impairment in GSIS caused by VGF suppression. Acute stimulation with either the adenylate cyclase activator, forskolin, or the phosphodiesterase inhibitor, isobutylmethylxanthine (IBMX), failed to restore the full secretory response of VGF knockdown cells to control levels, despite a clear enhancement in insulin secretion in response to these agents (Fig. 1C). Importantly, VGF suppression did not alter cAMP accumulation following either a glucose challenge or stimulation with forskolin (Fig S1A). Similarly, the GLP-1R agonist, exendin-4, also failed to rescue the GSIS defect accompanying VGF suppression (Fig. S1B). Furthermore, insulin release stimulated by direct membrane depolarization (tolbutamide or elevated KCl) under basal glucose

conditions remained significantly reduced following VGF suppression as compared to control cells (Fig. 1D). Elevated KCl in the presence of stimulatory glucose also failed to promote a full insulin secretory response in VGF knockdown cells (Fig. 1E).

Importantly, we did not observe any changes in cell viability (data not shown) or the expression levels of the exocytic or glucose uptake machinery (Fig. S2). Together, these data highlight a significant impairment in insulin secretion in response to VGF deficiency.

To explore the physiologically significance of the observations made in cultured cells, we generated a β-cell specific knockout of VGF using homozygous VGF floxed mice expressing the tamoxifen inducible MIP-CreERT transgene ($Vgf^{\text{flpflox/flpflox}}$; MIP-CreERT). Using this approach, islets isolated from tamoxifen-treated animals had a 70% decrease in VGF mRNA expression with a concomitant loss of VGF protein by immunoblot as compared to control animals treated with vehicle alone (Fig. 2A). The remaining VGF expression likely represents expression in islet α- and δ-cells as reported elsewhere (Cocco et al., 2007). Consistent with our siRNA knockdown studies, islets isolated from β-cell VGF KO (tamoxifen) animals showed a clear impairment in GSIS as compared to control islets from vehicle-treated animals (Fig. 2B). Furthermore, following a glucose challenge, β-cell VGF KO mice (tamoxifen) demonstrated an impaired glycemic excursion (Fig. 2C) in concert with a decrease in the plasma insulin response (Fig. 2D) as compared to control (vehicle) mice. No change in body weight (Fig. S1C) or insulin sensitivity (Fig. S1D) was observed. Together these data demonstrate that VGF plays a key role in regulating normal β-cell function.

VGF is necessary to maintain insulin granule stores

A recent publication documented a decrease in dense core secretory granule size in adrenal chromaffin cells from whole body VGF knockout mice (Fargali et al., 2014). We postulated that the strong effect of VGF suppression on GSIS may be related to differences in granule size and/or structure. We first examined insulin content in islets from β-cell VGF KO (tamoxifen) mice (Fig. 3A) and following VGF knockdown (siRNA) in 832/3 insulinoma cells (Fig. 3B). Here, we observed a significant decrease in insulin content upon loss of VGF in both isolated islets (Fig. 3A, compare to vehicle) and 832/3 cells (Fig. 3B, compare to SCR or mock). Next, we used electron microscopy to investigate secretory granules at the ultrastructural level in 832/3 cells following glucose stimulation. Morphometric analysis of electron micrographs (n = 60–65 per treatment; representative images shown in Fig. 3C) revealed a 25% decrease in the total number of dense core secretory granules in VGF knockdown cells (Fig. 3D). More specifically, loss of VGF coincided with a decrease in the frequency of granules larger than 8000 nm^2 (Fig. 3E). Further examination demonstrated a 33% decrease in ready-releasable granules, defined as granules 200 nm from the plasma membrane (Fig. 3F). Similar to the total granule pool, we observed a significant decrease in the frequency of large dense core granules proximal to the plasma membrane in VGF deficient cells (Fig. S3). These data highlight deficiencies in insulin content in VGF loss of function β-cells.

VGF suppression disrupts granule localization

To further examine potential effects of VGF on secretory granule size and composition, we used density gradient sedimentation to resolve insulin-containing granule fractions and associated granule markers, such as PC2 and VGF, from ER and trans-Golgi markers, GRP94 and TGN38, respectively (Fig. S4A). As shown in Figure 4A and consistent with data provided in Figure 3, we observed a significant depletion of the insulin granule pool in VGF siRNA-treated cells, as compared to control SCR siRNA-treated cells. Moreover, we also noted that insulin-containing granules from VGF knockdown cells migrated to less dense regions of the gradient than granules from control (SCR) cells, consistent with our ultrastructural data demonstrating that granules derived from VGF knockdown cells were typically smaller in size (Fig. 3E). In addition, fractions containing other granule markers such as PC2, which co-migrated with insulin, were also shifted toward less dense fractions in VGF siRNA-treated cells relative to SCR-siRNA treated control cells (Fig. 4A). We also examined sedimentation profiles of granule markers using the GRINCH insulinoma cell line, which contains a "superfolder" GFP-labeled proinsulin (pro-Cpep-SfGFP) that can be fully processed to mature insulin and C-peptide-SfGFP (Haataja et al., 2013). Using GFP as a marker for granules containing processed insulin (C-pep-SfGFP), we again observed a shift in granule sedimentation into less dense fractions from VGF siRNA knockdown cells as compared to SCR-siRNA treated control cells (Fig. 4B), with a similar shift for another granule marker chromogranin B (CgB).

From our ultrastructural data and sedimentation analysis, we observed a decrease in both the number and size of insulin-containing secretory granules in VGF deficient cells. Next, we examined the subcellular localization of insulin granules via immunostaining in 832/3 cells. In control cells (SCR siRNA), insulin was detected as punctate staining diffusely spread throughout the cytosol as expected for a granule protein (Fig. 4C). In contrast, VGF suppression resulted in a significant accumulation of insulin in a subcellular region that co-stained with the *trans*-Golgi marker, TGN46. We also investigated whether other granule markers such as chromogranins A and B (CgA and CgB) displayed altered localization in VGF deficient cells. Similar to insulin, CgA (Fig. S4B) and CgB (Fig. 4D) staining was primarily diffuse and punctate throughout the cytosol in control (SCR siRNA) cells, whereas in cells treated with VGF siRNAs, there was a significant accumulation of CgB and CgA staining at or near the TGN. Importantly we did not observe any changes in the localization of plasma membrane markers such as the *t*-SNARE, syntaxin 1A (Fig. S2C). Together these data highlight important distinctions in granule sedimentation and localization in VGF deficient cells and suggest that VGF is necessary for proper granule formation in the islet β-cell.

VGF suppression reduces proinsulin processing

Given the altered density, localization, and size of insulin granules in VGF deficient cells, we next investigated whether loss of VGF also impacts proinsulin synthesis and maturation to insulin. We first examined whether proinsulin biosynthesis was impaired in VGF knockdown cells using radioisotope tracer analysis. Here, 832/3 cells were pulse-labeled with [^{35}S]-methionine/cysteine under either basal (2.5 mM) or stimulatory (12 mM) glucose conditions. No differences were observed in total protein synthesis in response to either

glucose or siRNA treatment (Fig. S5). As expected, we observed an increase in glucose-stimulated proinsulin biosynthesis (Fig. 5A; compare 2.5 mM vs. 12 mM Glc) consistent with previously published data (Itoh and Okamoto, 1980, Permutt, 1974), with no differences in this response in VGF deficient cells as compared to control (SCR-treated and mock transfected) cells. Next, we measured proinsulin maturation during glucose stimulation in 832/3 cells treated with cycloheximide at various time points to prevent further protein synthesis. In this model, the half-life of proinsulin (either converted to insulin or released) is approximately 18–19 minutes (Fig. 5B; see SCR and mock controls). Following VGF suppression, we observed a striking delay in the disappearance of proinsulin with an almost two-fold increase in proinsulin half-life as compared to SCR siRNA and mock control cells (Fig. 5B; 33.8 min vs. 18.5 min, respectively). Consistent with this, we observed a marked increase in the ratio of proinsulin to total insulin (insulin + proinsulin) in islets derived from β-cell VGF KO animals (tamoxifen-treated) as compared to control (vehicle) islets (Fig. 5C) with similar results in our VGF knockdown insulinoma cell line (Fig 5D). These data demonstrate that the alterations in granule size and localization correspond to diminished maturation of granule cargo.

Loss of VGF impairs replenishment of insulin granule stores

Several studies have suggested that newly formed insulin granules are preferentially used for insulin secretion rather than older resident granules due to changes in granule mobility (Straub et al., 2004, Rhodes and Halban, 1987, Rorsman and Renstrom, 2003, Hao et al., 2005). We postulated that the strong effect of VGF suppression on insulin secretion may reflect a decrease in the ability to rapidly replenish secretion-competent insulin granules due to decreased granule formation and maturation. To test this, we first examined insulin secretion by perifusion of islets derived from wild-type (vehicle) and β-cell VGF KO (tamoxifen) animals. As shown in Figure 6A, we observed a clear reduction in glucose-stimulated insulin secretion in β-cell VGF KO islets, consistent with data presented in Figure 2B. Furthermore, β-cell VGF KO islets challenged with forskolin also had diminished insulin secretion (data not shown). Next, we separately interrogated first- and second-phase insulin secretion to determine whether either or both phases were impacted by loss of VGF. To do this, we examined first-phase insulin release by simulating ATP-mediated suppression of K_{ATP} channels via direct membrane depolarization. This was accomplished via a train of KCl stimulations at basal glucose followed by rest periods (12 min) of basal glucose alone. As shown in Fig. 6B, no significant difference was observed in response to three consecutive KCl challenges in islets isolated from β-cell VGF KO animals (tamoxifen) as compared to control islets (vehicle). To examine insulin release independent of the K_{ATP} channel (i.e. second-phase), we used diazoxide to prevent K_{ATP} channel closure in the presence of stimulatory glucose and elevated KCl. In these studies, we observed a marked impairment in insulin release in β-cell VGF KO islets (tamoxifen) (Fig. 6C), which worsened over time (Fig. 6D). Together these data demonstrate VGF is necessary for the sustained replenishment of insulin granules to maintain full insulin secretory capacity of the islet β-cell.

Discussion

Pancreatic islet β-cells are central regulators of whole animal fuel metabolism, coupling nutritional demands and uptake with insulin release. The maintenance of sufficient insulin stores to ensure glucose homeostasis requires the constant renewal of insulin-containing secretory granules (Rorsman and Renstrom, 2003). Current reports indicate that approximately 50–100 distinct proteins exist within the β-cell secretory granule (Hickey et al., 2009, Schvartz et al., 2012, Brunner et al., 2007), many of which have unknown functions in mediating granule formation and movement (Suckale and Solimena, 2010). While VGF has been described in dense core granules from multiple endocrine cell types (Ferri et al., 1992, Possenti et al., 1999, Gentile et al., 2004), the function of VGF, particularly in peripheral tissues, is not well understood. Studies of VGF function have been largely divided between characterizing the (pharmacological) actions of the secreted VGF-derived peptide fragments and examining the physiology of VGF deficient animals (reviewed in Bartolomucci et al., 2011, Levi et al., 2004, Salton et al., 2000). Work in adrenal medullary chromaffin cells suggests that VGF can function intracellularly as a granin protein, facilitating granulogenesis and interacting with granule cargo (Fargali et al., 2014). Here, we have expanded on that observation by highlighting a key role for VGF in promoting efficient formation of secretory granules in islet β-cells thereby providing insight into the role of VGF in maintaining islet β-cell function.

In this report, we show that loss of VGF has profound effects on stimulus-coupled insulin secretion. Suppression of VGF impaired β-cell responses to a series of secretagogues including glucose, agents that directly raise cAMP (forskolin, IBMX), a $G_{\alpha s}$-coupled peptide agonist (exendin-4) and direct membrane depolarization (KCl). Ultrastructural examination demonstrated that VGF knockdown cells contained fewer and smaller dense core secretory granules than control cells, which was further corroborated by equilibrium sedimentation analysis. Despite the decrease in insulin content induced by loss of VGF, simply normalizing insulin release to total insulin content did not resolve the apparent secretory deficit (Figs. 1A and 6). We propose that the decrease in secretory potential observed in VGF deficient cells is directly related to the reliance on newly synthesized granules for continued secretion (Straub et al., 2004, Rhodes and Halban, 1987, Rorsman and Renstrom, 2003, Hao et al., 2005).

Biphasic insulin release has been proposed to reflect mobilization of distinct pools of insulin granules (Curry et al., 1968, Henquin et al., 2002) with first-phase release utilizing granules pre-docked at the plasma membrane (Barg et al., 2002) and the second-phase requiring mobilization of additional granule stores (Renstrom et al., 1996). Careful examination of first- and second-phase insulin secretion from β-cell VGF KO islets revealed a profound impairment in second-phase secretion only, which may reflect distinct requirements of VGF for sustained secretion in response to more prolonged stimulation. We speculate that in the absence of diabetic stresses (hyperglycemia and insulin resistance), VGF deficient granules can accumulate and replenish granule stores in response to short exposure to stimulation, which allows the preservation of acute insulin release in response to direct membrane depolarization. In contrast, continuous stimulation results in defective insulin release in VGF KO cells due to a lag in granule replenishment. In support of this, granule cargo accumulated

at or adjacent to the *trans*-Golgi network in VGF knockdown cells with a concomitant rise in proinsulin content due to diminished hormone processing. Note that in cell lines, we did observe a decrease in insulin release in response to membrane depolarization at basal glucose; however, these experiments were conducted over a two hour time course, which may have sufficiently depleted granule stores in VGF knockdown cells. We propose that in the absence of VGF, the reduced efficiency of granule formation and/or trafficking may be inadequate to sustain a strong second-phase insulin response. How VGF coordinates this action is not known, but may involve direct association with other granin members as suggested by studies in PC12 cells (Fargali et al., 2014).

It is well appreciated that loss of insulin secretory capacity is the key event defining the transition from the prediabetic state to full-blown Type 2 diabetes (T2D). Reduced β-cell function and mass coupled with increasing insulin resistance in peripheral tissues results in a disparity between the available insulin supply and the demand for insulin signaling. In early stages of T2D, β-cell dysfunction is evident, with significant defects in both first- and second-phase insulin secretion (Ward et al., 1984, Gerich, 2002). This is accompanied by a reduction in mature dense core secretory granules (Masini et al., 2012, Like and Chick, 1970, Alarcon et al., 2016). Recent studies have demonstrated that islet β-cells from rodent models of T2D synthesize proinsulin at an astonishingly high rate (Alarcon et al., 2016) suggesting that proinsulin synthesis is not limiting; rather the storage of insulin becomes impaired due to downstream defects in granule formation and trafficking. In this model, the aberrant formation and storage of insulin granules leads to inappropriate segregation of granule cargo, insufficient proteolytic processing of prohormones, and the untimely release of insulin and proinsulin. Our studies suggest that loss of VGF or a VGF-regulated pathway could be involved in development of islet β-cell dysfunction in T2D. Further investigation into the role of granin proteins such as VGF in the packaging and storage of insulin into secretory granules may have important implications for understanding the pathogenesis of β-cell dysfunction.

Experimental Procedures

Cell culture and reagents

832/3 cells were cultured as previously described (Hohmeier et al., 2000). GRINCH cells expressing pro-C-pep-SfGFP were a kind gift of Dr. Peter Arvan (University of Michigan) (Haataja et al., 2013). Individual (Dharmacon) or SMARTpool (Dharmacon) siRNAs targeting rat VGF were transfected using Dharmafect I (Dharmacon) and cells assayed 72 h post-transfection. Mouse islets were isolated via collagenase V (Sigma) digestion and purified using Histopaque 1077 and 1119 (Sigma). Islets were cultured in RPMI supplemented with 10% fetal bovine serum and 1 % penicillin and streptomycin and maintained at 37°C in 5% CO_2. Cell culture reagents were from Life Technologies unless specified otherwise.

Animal studies

MIP-CreERT (B6.Cg-Tg(Ins1-cre/ERT)1Lphi/J) mice were provided by Dr. Louis Phillipson (University of Chicago) (Wicksteed et al.). $Vgf^{flpflox/flpflox}$ mice (Lin et al., 2015) were bred

with MIP-CreERT mice to generate heterozygous animals and then backcrossed for at least 8 generations to the $Vgf^{flpflox/flpflox}$ parental line. $Vgf^{flpflox/flpflox}$; MIP-CreERT mice at 6–8 weeks of age were injected i.p. with 3–5 mg tamoxifen dissolved in corn oil containing 5% ethanol or vehicle control on 5 consecutive days. 4–6 wks post-tamoxifen treatment, glucose tolerance was measured in 4–6 hr fasted mice given a 1.5 mg/g body weight glucose (i.p.) challenge. Insulin tolerance was measured in 2 hr fasted mice given a 1.0 mU/g body weight Humulin-R (Eli Lilly) injection (i.p.). Blood glucose was determined using either a BD or ReliOn glucometer. Plasma insulin was determined by ELISA (Mercodia). All animal protocols were approved by the Institutional Animal Use and Care Committee at either Duke University or the University of Iowa.

Glucose-stimulated insulin secretion

Insulin secretion was measured by static incubation of 832/3 cells as previously described (Hohmeier et al., 2000), in secretion assay buffer (SAB) containing 2.5mM Glc followed by 12 mM Glc for 2 h each at 37°C. The secretagogues KCl (35 mM), exendin-4 (20 nM), isobutylmethylxanthine (100 μM), and forskolin (500 nM) were included in the basal or stimulatory glucose conditions where indicated. Mouse islet insulin secretion was measured by static incubation of 15–20 islets in at least 5 replicate groups in SAB containing 2.5mM Glc or 16.7 mM Glc for 1 h at 37°C. Insulin was measured in SAB via RIA (Coat-a-Count kit; Siemens) or ELISA (rodent, 80-INSMR-CH10, ALPCO). Cells were lysed in RIPA buffer and total protein determined by BCA (Pierce). Insulin (rodent, 80-INSMR-CH10, ALPCO) and proinsulin (mouse, 80-PINSMS-E01; rat, PINSRT-E01, ALPCO) content were determined by ELISA from whole cell lysates. Proinsulin content was determined as the percentage of proinsulin relative to insulin + proinsulin.

Islet perifusion

Approximately 40 islets were perifused at 37°C using a BioRep Perifusion system with a flow rate of 100 μL per min. Perifusate was collected at 1–2 min intervals. Following stabilization of insulin release under basal (2.5 mM) glucose conditions (up to 32 min) islets were stimulated with various secretagogues (35 mM KCl, 16.7 mM Glc, 11.2 mM Glc + 100 μM diazoxide + 35 mM KCl) where indicated. For repeated stimulations, islets were stimulated at basal glucose (2.5 mM) with 35 mM KCl for 12 min followed by glucose (2.5 mM) alone for 12 min. Islets were collected from perifusion chambers and lysed in RIPA buffer. Insulin content of perifusate and cell lysate was determined by ELISA (ALPCO).

cAMP determination

For cAMP measurements, 832/3 cells were prepared as for insulin secretion assays, except the incubation at stimulatory glucose was for 15 min in the presence of 0.1mM isobuytlmethylxanthine (IBMX) as previously described (Stephens et al.). Cell extracts were assayed by ELISA (Biomedical Technologies, Inc.).

Immunoblot analysis

Clarified cell lysates were resolved on 4–12% NuPAGE gels (Life Technologies) and transferred to polyvinylidene fluoride (PVDF) or supported nitrocellulose membranes.

Membranes were probed with diluted antibodies raised against chromogranin A (rabbit, Abcam; goat, Santa Cruz), chromogranin B (rabbit, Abcam; goat, Santa Cruz), Munc18 (Cell Signaling), GFP (rabbit, Abcam), PC1 (rabbit, Abcam), PC2 (rabbit, Abcam), Rab3a (Sigma) SNAP25 (Cell Signaling), synaptotagmin 7 (Sigma), synaptotagmin 9 (Sigma), syntaxin 1 (Millipore), syntaxin 4 (Millipore), gamma-tubulin (Sigma), VAMP2 (Cell Signaling), or VGF (Sigma or polyclonal antisera supplied by Dr. Stephen Salton). Donkey anti-mouse (Invitrogen), goat-anti-rabbit (Licor), and donkey anti-goat (Rockland) antibodies coupled to IR-dye 680 or 800 were used to detect primary antibodies. Blots were developed using an Odyssey CLx Licor Instrument.

In situ immunofluorescence

832/3 cells 48 hrs post siRNA transfections were seeded at low density on HTB9 coated-slides (Hayes et al., 2017) and cultured overnight. Following treatments, cells were fixed in 10 % neutral-buffered formalin and incubated overnight with antibodies raised against insulin (Dako), chromogranin A (Abcam), chromogranin B (Abcam), and TGN46 (Abcam) as indicated. AlexaFluor conjugated secondary antibodies (Invitrogen) were used for detection. Cells were counterstained with DAPI (Sigma) and mounted using Fluorosave (Calbiochem). Images were captured using a Zeiss Axiophot microscope and analyzed by Fiji software.

Proinsulin biosynthesis

Following 1 hr incubation in SAB containing 2.5 mM Glc, cells were incubated for 40 min in fresh SAB containing either 2.5 mM or 12 mM Glc. Subsequently, cells were incubated for 20 min in SAB containing the respective basal or stimulatory glucose and 400 μCi of [^{35}S]-met/cys (MP Biomedical). Cells were lysed in RIPA and clarified lysates immunoprecipitated using (pro)insulin antibodies (Cell Signaling and Dako). Immunoprecipitated samples were resolved on Novex 16% Tricine gels (Life Technologies); aliquots of whole cell lysate were resolved on 4–12% NuPAGE gels (Life Technologies) for determination of total protein synthesis. Dried gels were exposed to phosphorimager screens and detected using a Typhoon Imager (GE Healthcare) and ImageQuant software (GE Healthcare).

Density gradient isolation of secretory granules

Cells were collected, washed in PBS, and disrupted using 15 strokes in a pre-chilled ball-bearing cell homogenizer (Isobiotec) with a 12 micron clearance in 10 mM MES pH 6.5, 1 mM MgSO$_4$, 1 mM EDTA, 0.3 M sucrose. Post-nuclear supernatants were layered atop 8–20% linear iodixanol (Optiprep; Sigma) gradients and resolved at 160,000 x g's in an SW41 for 16–18 hr. Fractions were manually collected by tube puncture. Iodixanol gradients were verified by absorbance at 340 nm. Insulin content was determined by ELISA (ALPCO) and normalized to the total protein loaded onto the gradient as determined by BCA. For immunoblots, total protein was TCA precipitated, resuspended in sample buffer (Thermo) and prepared as described above.

Ultrastructural studies

Following 1 hr incubation in SAB containing 2.5 mM Glc, cells were incubated for 30 min in fresh SAB containing 12 mM Glc. Cells were then washed and fixed in 2.5% glutaraldehyde in cacodylate buffer pH 7.3 for 0.5 h at 37°C. Cells were post-fixed in 1% OsO_4 and stained *en bloc* in 2% uranyl acetate. Samples were dehydrated using a graded alcohol series and resin embedded. Sections (50–100 nm) were imaged on a Philips EM420 electron microscope. Images (60–65 per group) were blinded and dense core secretory granules counted and sized using ImageJ (Fiji) software.

Statistical Analysis

Data are presented as the mean + S.E.M. For statistical significance determinations, data were analyzed by the two-tailed unpaired, Student's t test or by ANOVA with Bonferroni or Tukey post-hoc analysis for multiple group comparisons (GraphPad Prism). Nonlinear regression analysis was used to compare curve fits for proinsulin turnover studies (GraphPad Prism).

Supplementary Material

Refer to Web version on PubMed Central for supplementary material.

Acknowledgments

Abbreviations

Ex-4	exendin-4
Fsk	forskolin
Glc	glucose
GSIS	glucose-stimulated insulin secretion
i.p	intraperitoneal
IBMX	isobutylmethylxanthine
pIns	proinsulin
SAB	secretion assay buffer
Tm	tamoxifen
Tb	tolbutamide
T2D	Type 2 diabetes

References

ALARCON C, BOLAND BB, UCHIZONO Y, MOORE PC, PETERSON B, RAJAN S, RHODES OS, NOSKE AB, HAATAJA L, ARVAN P, MARSH BJ, AUSTIN J, RHODES CJ. Pancreatic beta-Cell Adaptive Plasticity in Obesity Increases Insulin Production but Adversely Affects Secretory Function. Diabetes. 2016; 65:438–50. [PubMed: 26307586]

ARVAN P, CASTLE D. Sorting and storage during secretory granule biogenesis: looking backward and looking forward. Biochem J. 1998; 332(Pt 3):593–610. [PubMed: 9620860]

BARG S, ELIASSON L, RENSTROM E, RORSMAN P. A subset of 50 secretory granules in close contact with L-type Ca2+ channels accounts for first-phase insulin secretion in mouse beta-cells. Diabetes. 2002; 51(Suppl 1):S74–82. [PubMed: 11815462]

BARTOLOMUCCI A, POSSENTI R, MAHATA SK, FISCHER-COLBRIE R, LOH YP, SALTON SR. The extended granin family: structure, function, and biomedical implications. Endocr Rev. 2011; 32:755–97. [PubMed: 21862681]

BRUNNER Y, COUTE Y, IEZZI M, FOTI M, FUKUDA M, HOCHSTRASSER DF, WOLLHEIM CB, SANCHEZ JC. Proteomics analysis of insulin secretory granules. Mol Cell Proteomics. 2007; 6:1007–17. [PubMed: 17317658]

CHUNG KN, WALTER P, APONTE GW, MOORE HP. Molecular sorting in the secretory pathway. Science. 1989; 243:192–7. [PubMed: 2911732]

COCCO C, BRANCIA C, PIRISI I, D'AMATO F, NOLI B, POSSENTI R, FERRI GL. VGF metabolic-related gene: distribution of its derived peptides in mammalian pancreatic islets. J Histochem Cytochem. 2007; 55:619–28. [PubMed: 17312015]

COOL DR, LOH YP. Carboxypeptidase E is a sorting receptor for prohormones: binding and kinetic studies. Mol Cell Endocrinol. 1998; 139:7–13. [PubMed: 9705069]

CURRY DL, BENNETT LL, GRODSKY GM. Dynamics of insulin secretion by the perfused rat pancreas. Endocrinology. 1968; 83:572–84. [PubMed: 4877098]

DIAZ-VERA J, CAMACHO M, MACHADO JD, DOMINGUEZ N, MONTESINOS MS, HERNANDEZ-FERNAUD JR, LUJAN R, BORGES R. Chromogranins A and B are key proteins in amine accumulation, but the catecholamine secretory pathway is conserved without them. FASEB J. 2012; 26:430–8. [PubMed: 21990378]

DIKEAKOS JD, REUDELHUBER TL. Sending proteins to dense core secretory granules: still a lot to sort out. J Cell Biol. 2007; 177:191–6. [PubMed: 17438078]

FARGALI S, GARCIA AL, SADAHIRO M, JIANG C, JANSSEN WG, LIN WJ, COGLIANI V, ELSTE A, MORTILLO S, CERO C, VEITENHEIMER B, GRAIANI G, PASINETTI GM, MAHATA SK, OSBORN JW, HUNTLEY GW, PHILLIPS GR, BENSON DL, BARTOLOMUCCI A, SALTON SR. The granin VGF promotes genesis of secretory vesicles, and regulates circulating catecholamine levels and blood pressure. FASEB J. 2014; 28:2120–33. [PubMed: 24497580]

FARGALI S, SCHERER T, SHIN AC, SADAHIRO M, BUETTNER C, SALTON SR. Germline ablation of VGF increases lipolysis in white adipose tissue. J Endocrinol. 2012; 215:313–22. [PubMed: 22942234]

FERRI GL, LEVI A, POSSENTI R. A novel neuroendocrine gene product: selective VGF8a gene expression and immuno-localisation of the VGF protein in endocrine and neuronal populations. Brain Res Mol Brain Res. 1992; 13:139–43. [PubMed: 1315910]

GENTILE F, CALI G, ZURZOLO C, CORTEGGIO A, ROSA P, CALEGARI F, LEVI A, POSSENTI R, PURI C, TACCHETTI C, NITSCH L. The neuroendocrine protein VGF is sorted into dense-core granules and is secreted apically by polarized rat thyroid epithelial cells. Exp Cell Res. 2004; 295:269–80. [PubMed: 15051509]

GERICH JE. Is reduced first-phase insulin release the earliest detectable abnormality in individuals destined to develop type 2 diabetes? Diabetes. 2002; 51(Suppl 1):S117–21. [PubMed: 11815469]

HAATAJA L, SNAPP E, WRIGHT J, LIU M, HARDY AB, WHEELER MB, MARKWARDT ML, RIZZO M, ARVAN P. Proinsulin intermolecular interactions during secretory trafficking in pancreatic beta cells. J Biol Chem. 2013; 288:1896–906. [PubMed: 23223446]

HAHM S, FEKETE C, MIZUNO TM, WINDSOR J, YAN H, BOOZER CN, LEE C, ELMQUIST JK, LECHAN RM, MOBBS CV, SALTON SR. VGF is required for obesity induced by diet, gold thioglucose treatment, and agouti and is differentially regulated in pro-opiomelanocortin- and neuropeptide Y-containing arcuate neurons in response to fasting. J Neurosci. 2002; 22:6929–38. [PubMed: 12177191]

HAHM S, MIZUNO TM, WU TJ, WISOR JP, PRIEST CA, KOZAK CA, BOOZER CN, PENG B, MCEVOY RC, GOOD P, KELLEY KA, TAKAHASHI JS, PINTAR JE, ROBERTS JL, MOBBS CV, SALTON SR. Targeted deletion of the Vgf gene indicates that the encoded secretory peptide precursor plays a novel role in the regulation of energy balance. Neuron. 1999; 23:537–48. [PubMed: 10433265]

HAO M, LI X, RIZZO MA, ROCHELEAU JV, DAWANT BM, PISTON DW. Regulation of two insulin granule populations within the reserve pool by distinct calcium sources. J Cell Sci. 2005; 118:5873–84. [PubMed: 16317050]

HAYES HL, PETERSON BS, HALDEMAN JM, NEWGARD CB, HOHMEIER HE, STEPHENS SB. Delayed apoptosis allows islet beta-cells to implement an autophagic mechanism to promote cell survival. PLoS One. 2017; 12:e0172567. [PubMed: 28212395]

HELLE KB. The chromogranins. Historical perspectives. Adv Exp Med Biol. 2000; 482:3–20. [PubMed: 11192591]

HENDY GN, LI T, GIRARD M, FELDSTEIN RC, MULAY S, DESJARDINS R, DAY R, KARAPLIS AC, TREMBLAY ML, CANAFF L. Targeted ablation of the chromogranin a (Chga) gene: normal neuroendocrine dense-core secretory granules and increased expression of other granins. Mol Endocrinol. 2006; 20:1935–47. [PubMed: 16556729]

HENQUIN JC, ISHIYAMA N, NENQUIN M, RAVIER MA, JONAS JC. Signals and pools underlying biphasic insulin secretion. Diabetes. 2002; 51(Suppl 1):S60–7. [PubMed: 11815460]

HICKEY AJ, BRADLEY JW, SKEA GL, MIDDLEDITCH MJ, BUCHANAN CM, PHILLIPS AR, COOPER GJ. Proteins associated with immunopurified granules from a model pancreatic islet beta-cell system: proteomic snapshot of an endocrine secretory granule. J Proteome Res. 2009; 8:178–86. [PubMed: 19055480]

HOHMEIER HE, MULDER H, CHEN G, HENKEL-RIEGER R, PRENTKI M, NEWGARD CB. Isolation of INS-1-derived cell lines with robust ATP-sensitive K+ channel-dependent and -independent glucose-stimulated insulin secretion. Diabetes. 2000; 49:424–30. [PubMed: 10868964]

HOSAKA M, SUDA M, SAKAI Y, IZUMI T, WATANABE T, TAKEUCHI T. Secretogranin III binds to cholesterol in the secretory granule membrane as an adapter for chromogranin A. J Biol Chem. 2004; 279:3627–34. [PubMed: 14597614]

ITOH N, OKAMOTO H. Translational control of proinsulin synthesis by glucose. Nature. 1980; 283:100–2. [PubMed: 6985712]

KIM T, TAO-CHENG JH, EIDEN LE, LOH YP. Chromogranin A, an "on/off" switch controlling dense-core secretory granule biogenesis. Cell. 2001; 106:499–509. [PubMed: 11525735]

KIM T, TAO-CHENG JH, EIDEN LE, LOH YP. Large dense-core secretory granule biogenesis is under the control of chromogranin A in neuroendocrine cells. Ann N Y Acad Sci. 2002; 971:323–31. [PubMed: 12438143]

LEVI A, FERRI GL, WATSON E, POSSENTI R, SALTON SR. Processing, distribution, and function of VGF, a neuronal and endocrine peptide precursor. Cell Mol Neurobiol. 2004; 24:517–33. [PubMed: 15233376]

LIKE AA, CHICK WL. Studies in the diabetic mutant mouse. II. Electron microscopy of pancreatic islets. Diabetologia. 1970; 6:216–42. [PubMed: 4914662]

LIN WJ, JIANG C, SADAHIRO M, BOZDAGI O, VULCHANOVA L, ALBERINI CM, SALTON SR. VGF and Its C-Terminal Peptide TLQP-62 Regulate Memory Formation in Hippocampus via a BDNF-TrkB-Dependent Mechanism. J Neurosci. 2015; 35:10343–56. [PubMed: 26180209]

MAHAPATRA NR, O'CONNOR DT, VAINGANKAR SM, HIKIM AP, MAHATA M, RAY S, STAITE E, WU H, GU Y, DALTON N, KENNEDY BP, ZIEGLER MG, ROSS J, MAHATA SK. Hypertension from targeted ablation of chromogranin A can be rescued by the human ortholog. J Clin Invest. 2005; 115:1942–52. [PubMed: 16007257]

MASINI M, MARSELLI L, BUGLIANI M, MARTINO L, MASIELLO P, MARCHETTI P, DE TATA V. Ultrastructural morphometric analysis of insulin secretory granules in human type 2 diabetes. Acta Diabetol. 2012; 49(Suppl 1):S247–52. [PubMed: 23184237]

MOIN AS, YAMAGUCHI H, RHEE M, KIM JW, TOSHINAI K, WAISE TM, NAZNIN F, MATSUO T, SASAKI K, MINAMINO N, YOON KH, NAKAZATO M. Neuroendocrine regulatory peptide-2 stimulates glucose-induced insulin secretion in vivo and in vitro. Biochem Biophys Res Commun. 428:512–7.

MUOIO DM, NEWGARD CB. Mechanisms of disease: molecular and metabolic mechanisms of insulin resistance and beta-cell failure in type 2 diabetes. Nat Rev Mol Cell Biol. 2008; 9:193–205. [PubMed: 18200017]

OBERMULLER S, CALEGARI F, KING A, LINDQVIST A, LUNDQUIST I, SALEHI A, FRANCOLINI M, ROSA P, RORSMAN P, HUTTNER WB, BARG S. Defective secretion of islet hormones in chromogranin-B deficient mice. PLoS One. 2010; 5:e8936. [PubMed: 20126668]

PAN H, NANNO D, CHE FY, ZHU X, SALTON SR, STEINER DF, FRICKER LD, DEVI LA. Neuropeptide processing profile in mice lacking prohormone convertase-1. Biochemistry. 2005; 44:4939–48. [PubMed: 15779921]

PERMUTT MA. Effect of glucose on initiation and elongation rates in isolated rat pancreatic islets. J Biol Chem. 1974; 249:2738–42. [PubMed: 4597460]

PETROCCHI-PASSERI P, CERO C, CUTARELLI A, FRANK C, SEVERINI C, BARTOLOMUCCI A, POSSENTI R. The VGF-derived peptide TLQP-62 modulates insulin secretion and glucose homeostasis. J Mol Endocrinol. 2015; 54:227–39. [PubMed: 25917832]

POSSENTI R, RINALDI AM, FERRI GL, BORBONI P, TRANI E, LEVI A. Expression, processing, and secretion of the neuroendocrine VGF peptides by INS-1 cells. Endocrinology. 1999; 140:3727–35. [PubMed: 10433233]

RENSTROM E, ELIASSON L, BOKVIST K, RORSMAN P. Cooling inhibits exocytosis in single mouse pancreatic B-cells by suppression of granule mobilization. J Physiol. 1996; 494(Pt 1):41–52. [PubMed: 8814605]

RHODES CJ, HALBAN PA. Newly synthesized proinsulin/insulin and stored insulin are released from pancreatic B cells predominantly via a regulated, rather than a constitutive, pathway. J Cell Biol. 1987; 105:145–53. [PubMed: 3301864]

RORSMAN P, RENSTROM E. Insulin granule dynamics in pancreatic beta cells. Diabetologia. 2003; 46:1029–45. [PubMed: 12879249]

SALTON SR, FERRI GL, HAHM S, SNYDER SE, WILSON AJ, POSSENTI R, LEVI A. VGF: a novel role for this neuronal and neuroendocrine polypeptide in the regulation of energy balance. Front Neuroendocrinol. 2000; 21:199–219. [PubMed: 10882540]

SCHVARTZ D, BRUNNER Y, COUTE Y, FOTI M, WOLLHEIM CB, SANCHEZ JC. Improved characterization of the insulin secretory granule proteomes. J Proteomics. 2012; 75:4620–31. [PubMed: 22569486]

SEVERINI C, CIOTTI MT, BIONDINI L, QUARESIMA S, RINALDI AM, LEVI A, FRANK C, POSSENTI R. TLQP-21, a neuroendocrine VGF-derived peptide, prevents cerebellar granule cells death induced by serum and potassium deprivation. J Neurochem. 2008; 104:534–44. [PubMed: 18173805]

STEPHENS SB, SCHISLER JC, HOHMEIER HE, AN J, SUN AY, PITT GS, NEWGARD CB. A VGF-derived peptide attenuates development of type 2 diabetes via enhancement of islet beta-cell survival and function. Cell Metab. 16:33–43.

STRAUB SG, SHANMUGAM G, SHARP GW. Stimulation of insulin release by glucose is associated with an increase in the number of docked granules in the beta-cells of rat pancreatic islets. Diabetes. 2004; 53:3179–83. [PubMed: 15561948]

SUCKALE J, SOLIMENA M. The insulin secretory granule as a signaling hub. Trends Endocrinol Metab. 2010; 21:599–609. [PubMed: 20609596]

TRANI E, GIORGI A, CANU N, AMADORO G, RINALDI AM, HALBAN PA, FERRI GL, POSSENTI R, SCHININA ME, LEVI A. Isolation and characterization of VGF peptides in rat brain. Role of PC1/3 and PC2 in the maturation of VGF precursor. J Neurochem. 2002; 81:565–74. [PubMed: 12065665]

VAN DEN POL AN, DECAVEL C, LEVI A, PATERSON B. Hypothalamic expression of a novel gene product, VGF: immunocytochemical analysis. J Neurosci. 1989; 9:4122–37. [PubMed: 2556505]

WARD WK, BOLGIANO DC, MCKNIGHT B, HALTER JB, PORTE, DJR. Diminished B cell secretory capacity in patients with noninsulin-dependent diabetes mellitus. J Clin Invest. 1984; 74:1318–28. [PubMed: 6384269]

WASMEIER C, BRIGHT NA, HUTTON JC. The lumenal domain of the integral membrane protein phogrin mediates targeting to secretory granules. Traffic. 2002; 3:654–65. [PubMed: 12191017]

WATSON E, FARGALI S, OKAMOTO H, SADAHIRO M, GORDON RE, CHAKRABORTY T, SLEEMAN MW, SALTON SR. Analysis of knockout mice suggests a role for VGF in the control of fat storage and energy expenditure. BMC Physiol. 2009; 9:19. [PubMed: 19863797]

WATSON E, HAHM S, MIZUNO TM, WINDSOR J, MONTGOMERY C, SCHERER PE, MOBBS CV, SALTON SR. VGF ablation blocks the development of hyperinsulinemia and hyperglycemia in several mouse models of obesity. Endocrinology. 2005; 146:5151–63. [PubMed: 16141392]

WICKSTEED B, BRISSOVA M, YAN W, OPLAND DM, PLANK JL, REINERT RB, DICKSON LM, TAMARINA NA, PHILIPSON LH, SHOSTAK A, BERNAL-MIZRACHI E, ELGHAZI L, ROE MW, LABOSKY PA, MYERS MG JR, GANNON M, POWERS AC, DEMPSEY PJ. Conditional gene targeting in mouse pancreatic ss-Cells: analysis of ectopic Cre transgene expression in the brain. Diabetes. 59:3090–8. [PubMed: 20802254]

Highlights

- β-cell KO of VGF results in impaired glucose tolerance

- Loss of β-cell VGF strongly impairs stimulus-coupled insulin secretion

- VGF contributes to efficient exit of granule cargo from the *trans*-Golgi network

- VGF facilitates replenishment of insulin stores following nutrient stimulation
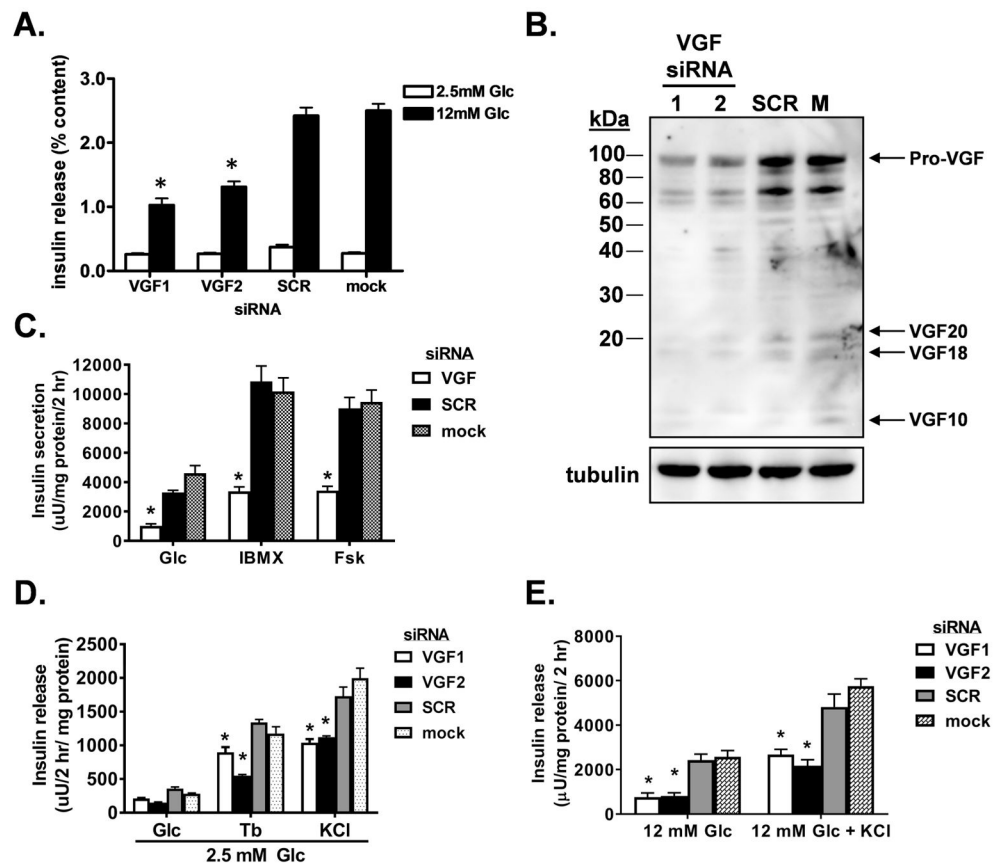
Figure 1. Insulin release in response to multiple stimuli is impaired by siRNA-mediated suppression of VGF

832/3 cells were transfected with individual rat VGF siRNA duplexes (VGF1, VGF2), a mixture of VGF duplexes (VGF; SMARTpool), non-targeting control duplex (SCR), or mock transfected as indicated. (**A**) GSIS was measured by static incubation in media containing 2.5 mM Glc and 12 mM Glc for 2 h each and normalized to insulin content. (**B**) Immunoblot analysis of whole cell lysates. (**C**) Insulin secretion was measured in cells stimulated with glucose (12 mM) alone or in concert with forskolin (0.5 μM) or isobutylmethylxanthine (100 μM) as indicated. (**D**) Insulin release was measured at 2.5 mM Glc in the presence or absence of tolbutamide (200 μM) or KCl (35 mM). (**E**) Insulin release was measured at 12 mM Glc in the presence or absence of KCl (35 mM). (**A, C–E**) Data represent the mean ± S.E.M of at least 3 independent experiments. * p 0.05 as compared to SCR siRNA- or mock-transfected cells.
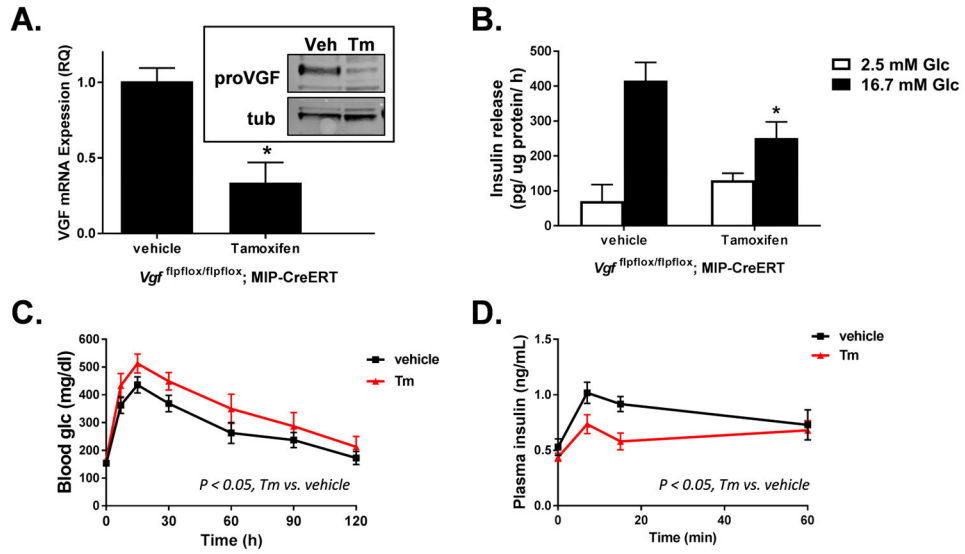
Figure 2. β-cell specific knockout of VGF in mice causes impaired glucose-stimulated insulin secretion

Male $Vgf^{\text{flpflox/flpflox}}$; MIP-CreERT mice (6–8 weeks of age) were injected (i.p.) with either vehicle (corn oil) or tamoxifen (Tm) as indicated and analyzed 4–6 weeks post-tamoxifen. (**A**) Quantitation of mRNA by real time PCR and immunoblot analysis (inset) of isolated islets (n = 3–4 mice per group). (**B**) GSIS was measured in isolated islets by static incubation in media containing 2.5 mM Glc or 16.7 mM Glc for 1 hr each (n = 5 mice per group). (**C**, **D**) Fasted mice were injected (i.p.) with a 1.5 mg/g bw glucose challenge (n = 8–10 per group). Blood glucose (**C**) and plasma insulin (**D**) were measured at the indicated times. (**A**, **C–D**) Data represent the mean ± S.E.M. * p   0.05 as compared to vehicle-treated animals.
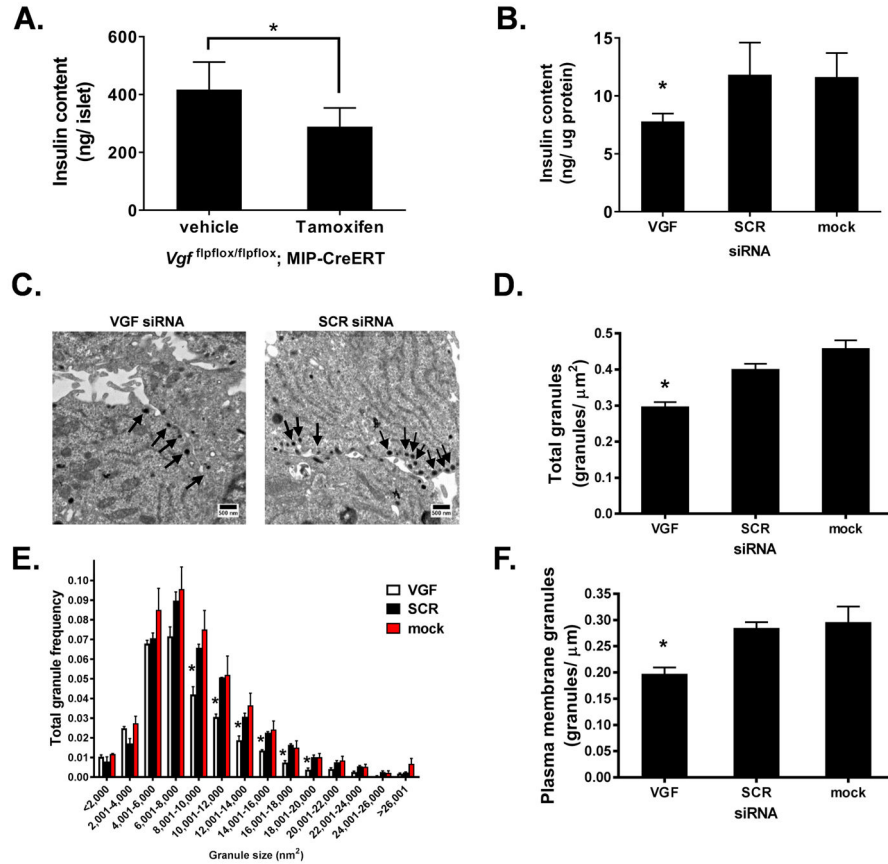
Figure 3. VGF suppression reduces secretory granule number and size

(**A**) Insulin content was determined from islets isolated from control (vehicle) and β-cell VGF KO (tamoxifen; Tm) mice. (**B**–**F**) 832/3 cells were transfected with rat VGF siRNA duplexes (SMARTpool), non-targeting control duplex (SCR), or mock transfected as indicated. (**B**) Insulin content was determined from whole cell lysates. (**C**–**F**) 832/3 cells were treated with 2.5 mM Glc for 1 hr followed by 12 mM Glc for 30 minutes and processed for electron microscopy. (**C**) Representative electron micrographs with arrows indicating dense core granules. (**D**) Total number of dense core granules normalized to total cell area. (**E**) Frequency distribution of binned total granule sizes. (**F**) Number of granules within 200 nm of the plasma membrane normalized to linear plasma membrane surface. Data represent the mean ± S.E.M of n = 6 mice per group (**A**) or 3 independent experiments (**B**, **D**–**F**). * p 0.05 as compared to control (vehicle) islets (**A**, unpaired ttest); or SCR siRNA- or mock-transfected cells (**B**, **D**, **F**; one-way ANOVA, Tukey post-test; **E**, two-way ANOVA, Bonferroni post-test).
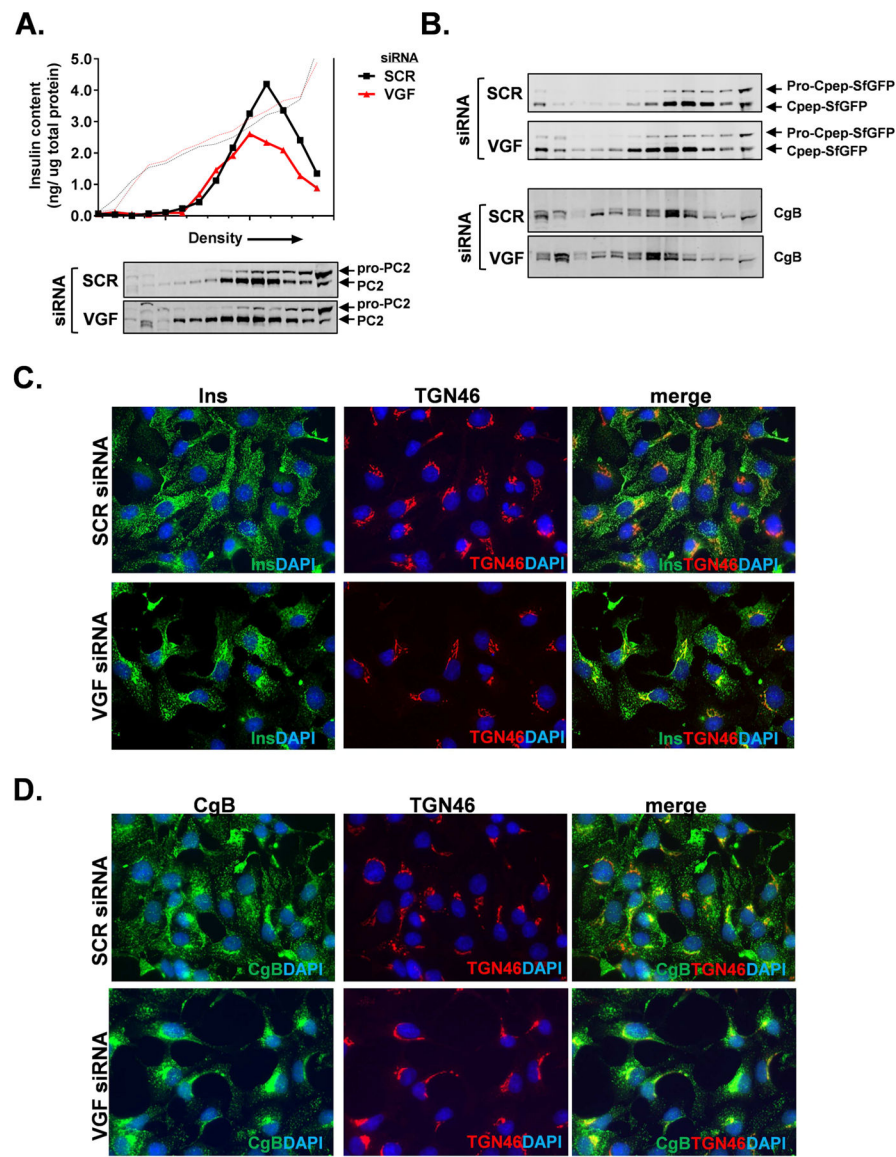
Figure 4. Granule cargo is retained in the *trans*-Golgi network following VGF knockdown
832/3 cells (**A**, **C**, **D**) or GRINCH (**B**) cells were transfected with rat VGF siRNAs duplexes (SMARTpool) or a non-targeting control duplex (SCR). (**A**, **B**) Cells were treated with 2.5 mM Glc for 1 hr followed by 12 mM Glc for 30 minutes and lysates resolved on 8–20% iodixanol gradients. (**A**) Representative chromatograph of insulin-containing secretory granule fractions is shown (arrow indicates direction of increasing density). Solid line represents insulin; dotted line represents gradient density. (**A**, **B**) Immunoblots of gradient fractions are shown. (**C**) Immunostaining of insulin (green) relative to TGN46 (red) counterstained with DAPI (blue). (**D**) Immunostaining of CgB (green) relative to TGN46 (red) counterstained with DAPI (blue).
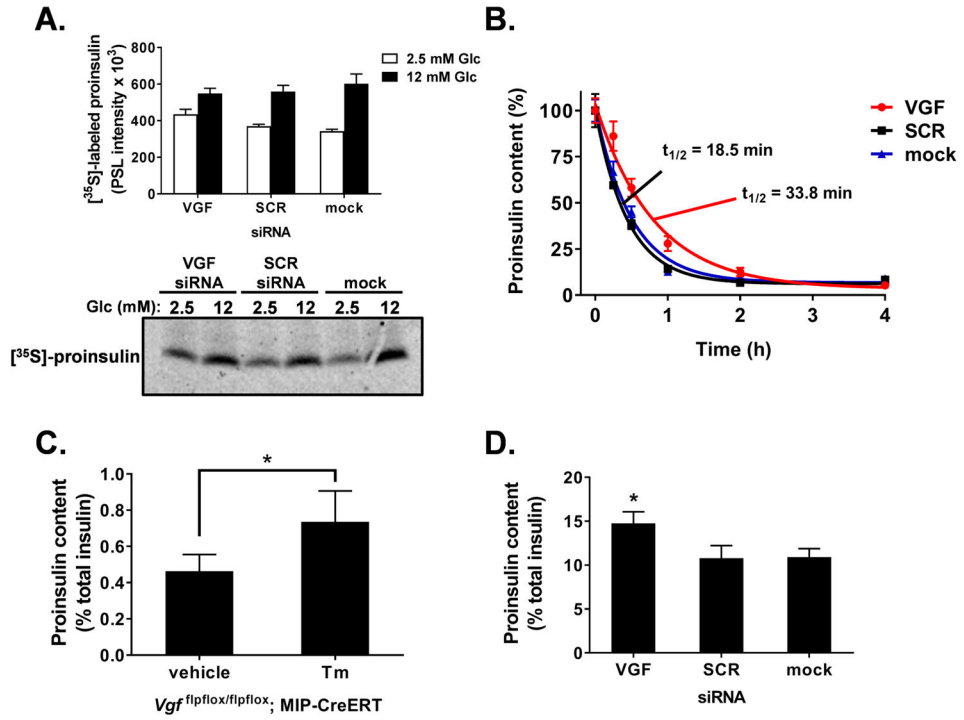
Figure 5. Delayed proinsulin processing in VGF deficient cells

(**A**, **B**, **D**) 832/3 cells were transfected with rat VGF siRNAs (SMARTpool), a non-targeting control siRNA (SCR), or mock transfected as indicated. (**A**) Cells were cultured in 2.5 mM or 12 mM Glc as indicated and pulse labeled with [^{35}S]-methionine/cysteine. Newly synthesized proinsulin was immunoprecipitated and quantified. (**B**) Cells were stimulated with Glc (12 mM) for 4 hrs and treated with cycloheximide (100 μM) at the indicated times. Proinsulin content was determined from whole cell lysates. Nonlinear regression analysis (GraphPad) was used to determine curve fits and proinsulin half-life. The ratio of proinsulin to total insulin (insulin + proinsulin) was determined using whole cell lysates from islets (**C**) isolated from control (vehicle) and β-cell VGF KO (tamoxifen) mice as indicated in the experimental methods section or 832/3 cells (**D**). Data represent the mean ± S.E.M. of three independent experiments (**A**, **B**, **D**) or n = 6 mice per group (**C**). * p ≤ 0.05 as compared to SCR siRNA-or mock-transfected cells (**A**, **D**) or islets derived from vehicle-treated animals (**C**).
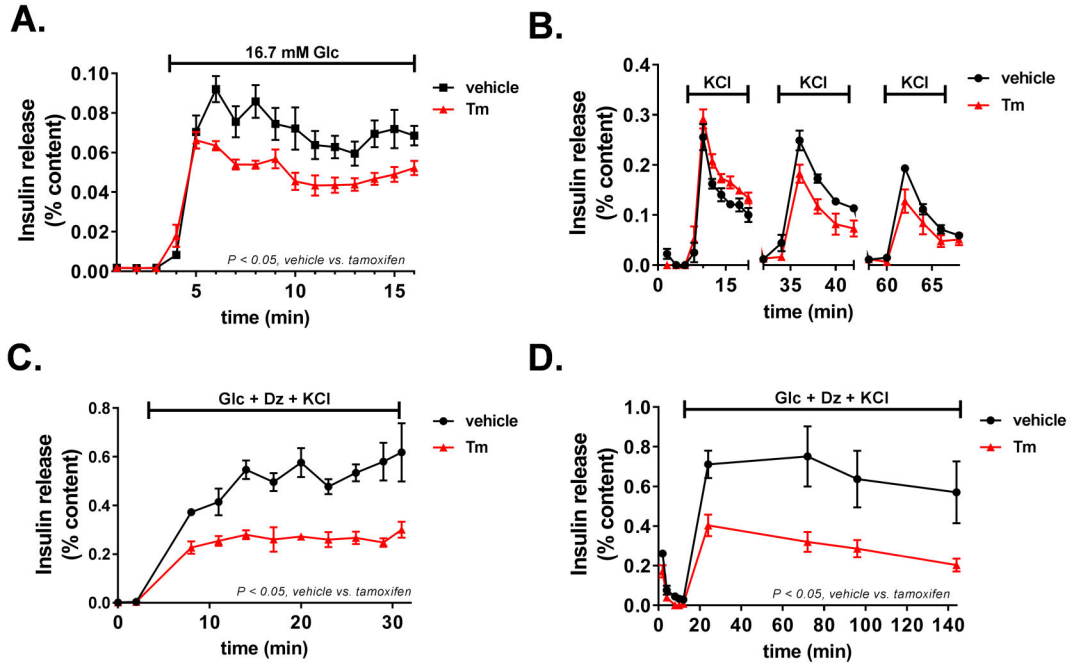
Figure 6. Loss of VGF impairs sustained insulin secretion
Islets were isolated from control (vehicle) and β-cell VGF KO (tamoxifen) mice as indicated in the experimental methods section. Insulin secretion profiles of perifused islets following stabilization at basal (2.5 mM) glucose are shown. (**A**) Islets were stimulated for 16 min at 16.7 mM Glc. (**B**) Islets were stimulated for 12 min with KCl (35 mM) at basal (2.5 mM) glucose followed by 12 min at basal glucose in the absence of KCl and repeated twice. (**C**, **D**) Islets were stimulated with a cocktail containing 11.2 mM Glc, 100 μM diazoxide (Dz), and 35 mM KCl for the indicated times. Data represent the mean ± S.E.M. (n = 4–6 mice per treatment). p < 0.05 tamoxifen vs. vehicle control.